

Assessing Stability of CERES-FM3 Daytime Longwave Unfiltered Radiance with AIRS Radiances

XIANGLEI HUANG

Department of Atmospheric, Oceanic, and Space Sciences, University of Michigan, Ann Arbor, Michigan

NORMAN G. LOEB

Radiation and Climate Branch, NASA Langley Research Center, Hampton, Virginia

HUIWEN CHUANG

Department of Atmospheric, Oceanic, and Space Sciences, University of Michigan, Ann Arbor, Michigan

(Manuscript received 12 April 2011, in final form 9 September 2011)

ABSTRACT

Clouds and the Earth's Radiant Energy System (CERES) daytime longwave (LW) radiances are determined from the difference between a total (TOT) channel (0.3–200 μm) measurement and a shortwave (SW) channel (0.3–5 μm) measurement, while nighttime LW radiances are obtained directly from the TOT channel. This means that a drift in the SW channel or the SW portion of the TOT channel could impact the daytime longwave radiances, but not the nighttime ones. This study evaluates daytime and nighttime CERES LW radiances for a possible secular drift in CERES LW observations using spectral radiances observed by Atmospheric Infrared Sounder (AIRS). By examining the coincidental AIRS and CERES Flight Model 3 (FM3) measurements over the tropical clear-sky oceans for all of January and July months since 2005, a secular drift of about $-0.11\% \text{ yr}^{-1}$ in the daytime CERES-FM3 longwave unfiltered radiance can be identified in the CERES Single Scanner Footprint (SSF) Edition 2 product. This provides an upper-bound estimation for the drift in daytime outgoing longwave radiation, which is approximately $-0.323 \text{ W m}^{-2} \text{ yr}^{-1}$. This estimation is consistent with the independent assessment concluded by the CERES calibration team. Such secular drift has been greatly reduced in the latest CERES SSF Edition 3 product. Comparisons are conducted for the CERES window channel as well, and it shows essentially no drift. This study serves as a practical example illustrating how the measurements of spectrally resolved radiances can be used to help evaluate data products from other narrowband or broadband measurements.

1. Introduction

As the successor of the Earth Radiation Budget Experiment (ERBE), the Clouds and the Earth's Radiant Energy System (CERES) plays a pivotal role in the continuation of monitoring the top-of-atmosphere (TOA) radiation budget (Wielicki et al. 1996; Loeb et al. 2007, 2009). CERES instruments consist of two broadband channels (a total channel and a shortwave channel) and one narrowband channel. The total (TOT) channel measures radiation from 0.3 to 200 μm and the shortwave

(SW) channel measures between 0.3 and 5 μm . The narrowband channel is the thermal IR window (WN; 8.1–11.8 μm) channel. The digital count recorded by each channel is first converted to calibrated "filtered" radiances, which is the convolution of the actual radiances intercepted by the optics and the spectral response function of each channel. An "unfiltering" algorithm is then applied to obtain the "unfiltered" radiances, that is, the actual radiances prior to entering the optics (Loeb et al. 2001). The TOA flux is then estimated from the unfiltered radiances using empirically derived angular distribution models (ADMs; Loeb et al. 1999, 2005). During the nighttime periods, the unfiltered TOT radiances are the longwave (LW) unfiltered radiances (i.e., the broadband radiance emitted by our climate system). During the daytime, the LW unfiltered radiances are the

Corresponding author address: Dr. Xianglei Huang, 2455 Hayward Street, Department of Atmospheric, Oceanic, and Space Sciences, University of Michigan, Ann Arbor, MI 48109-2143.
E-mail: xianglei@umich.edu

differences between the unfiltered TOT and SW radiances. Therefore, any secular drift that affects the SW channel or the SW portion of the TOT channel will eventually propagate to the estimation of daytime unfiltered LW radiances, and consequently to the estimation of daytime outgoing longwave radiation (OLR), but not to the nighttime counterparts. Such a SW drift and its impact on the trend of OLR have been shown before for the Earth Radiation Budget Satellite (ERBS) instrument (Wong et al. 2006) when decadal OLR trends have been carefully examined.

A spaceborne thermal IR spectrometer that measures the spectrally resolved radiances over a large portion of the longwave spectrum is not affected by solar radiation. Thus, when a thermal IR spectrometer and CERES are aboard the same satellite, coincident measurements can provide quantitative insights about the relative drift, if any, of daytime LW unfiltered radiances with respect to the nighttime ones. AIRS (Atmospheric Infrared Sounder; Aumann et al. 2003; Chahine et al. 2006) was aboard *Aqua*, together with two CERES instruments—Flight Models 3 and 4 (FM3 and FM4, respectively)—which gives us an opportunity to explore this approach. For comparison, we can also evaluate the CERES window channel radiances with the same approach. Because WN unfiltered radiance is not dependent on daytime SW measurements, no drift should be expected. This serves as an independent check of our analysis methodology.

The sections below are organized as follows. Section 2 describes the satellite datasets and methodology that we employ in this study. The main results are presented in section 3, followed by conclusions and discussions in section 4.

2. Dataset and collocation

a. CERES and AIRS datasets

Two CERES instruments, FM3 and FM4, were aboard the National Aeronautics and Space Administration (NASA) *Aqua* satellite. The CERES datasets used in this study are the *Aqua* CERES Single Satellite Footprint (SSF) TOA/Surface Fluxes and Clouds Editions 2 (Loeb et al. 2005) and 3. In Edition 2, time-dependent changes in the shortwave response of the total channel are derived using observations of deep convective clouds by all three channels of the instruments (Priestley et al. 2011). The idea is to adjust the SW portion of the TOT spectral response so that there is a “balance” between the SW channel and the SW portion of the TOT channel to yield an unbiased daytime LW radiance. Unfortunately, while this method works well for deep convective clouds,

a day–night LW bias still occurs for all-sky conditions. In Edition 3, a new algorithm (Loeb et al. 2012, hereafter LOE) is used that includes wavelength-dependent changes in the SW and SW portion of the TOT channel spectral response. The coefficients in the new algorithm are derived from clear-sky scenes over the oceans, and the algorithm is based on an expression of the loss of transmission with wavelength in the SW part only (details can be found in the appendix of LOE). Corrections to the SW portion of the TOT spectral response function are derived in order to remove any drift with time in the day–night LW against the day–night WN radiance relationship.

The planned operational modes for CERES are that, at any given time, one CERES instrument is placed in a cross-track scanning mode and the other is in either a rotating azimuth scanning or a programmable azimuth plane mode. The CERES FM4 shortwave radiometer stopped functioning in March 2005. Since then, it has not been able to provide daytime longwave radiances, and both instruments have been placed in the cross-track scanning mode. Therefore, in this study we will examine the FM3 instrument only.

AIRS is an infrared grating array spectrometer aboard NASA’s *Aqua* satellite (Aumann et al. 2003), operating in cross-track scanning mode and recording spectra at 2378 channels in three bands, that is, 3.74–4.61, 6.20–8.22, and 8.8–15.4 μm , with a resolving power ($\nu/\Delta\nu$) of 1200. The nadir-view CERES and AIRS footprints are 20 and 13.5 km, respectively. The AIRS in-flight calibrations have shown a radiometric accuracy of 0.3 K or higher for a 250-K brightness temperature target (Pagano et al. 2003) and a spectral accuracy of ~ 0.01 of the full width at half maximum of each channel (Gaiser et al. 2003). AIRS has also demonstrated excellent stability: Aumann et al. (2006) estimated the accuracy to be better than 200 mK and the stability to be better than 16 mK yr^{-1} , which is equivalent to 0.71 W m^{-2} or less for accuracy and 0.057 W m^{-2} or less per year for stability. Using longer AIRS time series, Aumann and Pagano (2008) updated the stability estimate to ~ 4 mK yr^{-1} . AIRS measures 2.9 million spectra per day and achieves global coverage within 2 days.

In this study we use the AIRS level-1B geolocated and calibrated radiances. Only channels recommended by the AIRS team for level-2 retrieval purposes are used. AIRS radiances from the near-IR band (3.74–4.61 μm) are not used for the reason that they can be affected by daytime solar radiation. Data are then further screened with a strict quality control procedure to exclude possible bad spectra, as done in Huang and Yung (2005).

b. Collocation strategy

The collocated AIRS and CERES-FM3 measurements are needed to ensure rigorous comparisons. The collocation criteria are identical to those used in Huang et al. (2008) and Huang et al. (2010), namely, 1) the time interval between AIRS and CERES observations is within 8 s, and 2) the distance between the center of an AIRS footprint and that of a CERES footprint on the surface is less than 3 km. These two criteria ensure that at least 50% of the AIRS footprint is within the CERES field of view, even if the scan angle goes to $\pm 45^\circ$. In practice, we only use AIRS data with scan angles within $\pm 45^\circ$. Figure 1a shows a scatterplot of collocated CERES unfiltered window channel radiances and AIRS radiances integrated over the same spectral range¹ over desert scenes in July 2005. Data points from both nighttime and daytime observations are lined up closely around a slope. Correlation coefficients for the nighttime and daytime observations are 0.997 and 0.998, respectively. Figure 1b is the corresponding scatterplot for collocated CERES unfiltered LW radiances and AIRS radiances integrated over its longwave portion (i.e., 650–1620 cm^{-1}). The correlation coefficients for the nighttime and daytime observations are 0.967 and 0.987, respectively. Thus, though there is a little bit more spread than data points in Fig. 1a, those in Fig. 1b are still tightly clustered together.

3. Analysis and results

a. Methodology

Motivated by previous studies that used narrowband radiance observation to estimate the outgoing longwave flux (Ellingson et al. 1989; Lee et al. 2004, 2007), a linear regression and prediction approach is employed to detect and assess the secular change of daytime CERES LW unfiltered radiances with respect to the nighttime counterparts. First, AIRS nighttime observations are regressed onto the coincidental CERES nighttime observations via

$$I_{\text{LW_CERES}} = \sum_{j=1}^6 a_j I_{\text{AIRS}} + b, \quad (1)$$

¹ Note the AIRS instrument has no full coverage for this spectral range, which explains why the AIRS integrated radiance is always smaller than the CERES WN unfiltered radiance. AIRS covers ~65% of the spectral range of the CERES WN channel and ~45% of the spectral range of the CERES LW channel.

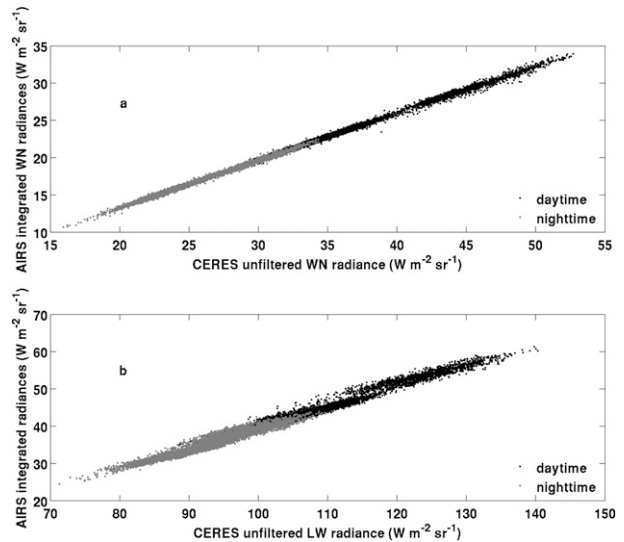


FIG. 1. (a) Scatterplots of CERES window channel radiances (Edition 2) vs collocated AIRS radiances integrated over the same spectral region (8.1–11.8 μm) over the clear-sky dark desert in July 2005. Nighttime (gray dots) and daytime (black dots) observations are shown. Note that AIRS does not have full coverage over this spectral region, which accounts for the AIRS integrated radiances always being smaller than their CERES counterparts. (b) As in (a), but for the AIRS radiances integrated over the longwave spectral region vs the collocated CERES unfiltered LW radiance. Note AIRS has no coverage between 0 and 650 cm^{-1} , which explains why the AIRS integrated radiances are always much smaller than their CERES counterparts on this plot.

where a_j and b are regression coefficients to be determined, $I_{\text{LW_CERES}}$ is the CERES LW unfiltered radiances, I_{AIRS} is the integration of AIRS radiances over all qualified AIRS channels in the j th band, that is,

$$I_{\text{AIRS}} = \sum_{v_i \in V_j} I_{\text{AIRS}}(v_i) dv_i, \quad (2)$$

where v_i is the frequency of the i th AIRS channel $dv_i \cong 2400/v_i$, and V_j is one of following six spectral bands: 640–800 cm^{-1} (CO_2 band), 800–900 or 1070–1200 cm^{-1} (atmospheric window regions), 900–990 cm^{-1} (window region with CO_2 hot bands), 990–1070 cm^{-1} (ozone band), 1200–1400 cm^{-1} (N_2O band, CH_4 Q branch, and tail of H_2O v_2 band), or 1400–1620 cm^{-1} (H_2O v_2 band). Once the regression coefficients (a_j , b) are obtained, they can be used to predict the LW unfiltered radiances (I_{est}) based on AIRS radiances for both daytime and nighttime observations. The relative difference between $I_{\text{LW_CERES}}$ and I_{est} for each collocated observation is

$$\text{rdiff} = \frac{I_{\text{LW_CERES}} - I_{\text{est}}}{I_{\text{est}}}. \quad (3)$$

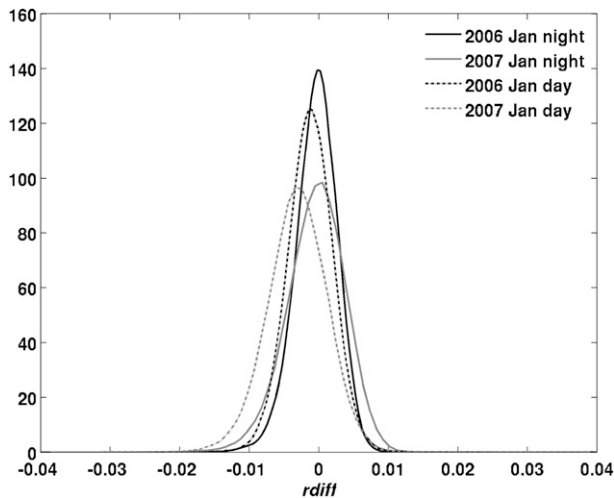


FIG. 2. The PDF of rdiff as defined in the context. The rdiff describes the fractional difference between CERES LW unfiltered radiance and LW radiance estimated from the collocated AIRS radiances using regression coefficients derived from nighttime observation alone. Four PDFs shown here are based on CERES Edition 2 data of January 2006 (black curves) and 2007 (gray curves). The rdiff of nighttime (solid lines) and daytime (solid-dashed lines) data are shown.

For each individual month, (a_j, b) are derived using nighttime observations alone, and then they are used to compute the probability distribution functions (PDFs) of rdiff for daytime and nighttime observations, respectively. While the PDFs of rdiff could be different for daytime and nighttime because of the diurnal variations of water substances and temperatures, such a day–night contrast in rdiff should not change appreciably with time. If a drift in time is observed, it is assumed to be due to a drift in the daytime I_{LW_CERES} with respect to its nighttime counterpart over the same period, because the regression coefficients are always derived from the nighttime observations in the same month. The 4 mK yr^{-1} stability of the AIRS instrument is equivalent to $\sim 0.0016\%$ drift per year (assume a 250-K blackbody object). Therefore, as long as the drift of rdiff is much larger than this value, the contribution of the AIRS stability to the drift can be neglected.

Examples of regression and PDFs of rdiff are shown in Fig. 2 for collocated AIRS and CERES-FM3 observations (Edition 2) over the tropical clear-sky oceans in January 2006 and January 2007. A CERES field of view is deemed as clear sky if the coincident Moderate Resolution Imaging Spectroradiometer (MODIS) pixel-level cloud coverage within the CERES field of view (FOV) is no more than 0.1%. As expected, the PDFs of nighttime rdiff are approximately Gaussian curves and their means are -0.0080 and -0.0040 for January 2006 and January 2007, respectively. For the daytime, the

TABLE 1. CERES unfiltered longwave broadband radiances averaged over clear-sky oceans between 30°S and 30°N for January 2006 and 2007 and July 2005–07, the Januaries and Julys that the FM3 operated in cross-track scanning mode. The standard deviation is given as well. Upper rows are CERES Edition 2 statistics and lower rows are CERES Edition 3 statistics.

	Daytime ($\text{W m}^{-2} \text{sr}^{-1}$)	Nighttime ($\text{W m}^{-2} \text{sr}^{-1}$)
January 2006	96.52 ± 3.54	96.18 ± 3.79
	96.66 ± 3.55	96.68 ± 3.81
January 2007	96.78 ± 3.82	96.13 ± 4.08
	96.91 ± 3.81	96.56 ± 4.10
July 2005	97.08 ± 3.89	96.45 ± 3.89
	97.04 ± 3.83	96.78 ± 3.87
July 2006	97.05 ± 3.77	96.70 ± 3.79
	97.04 ± 3.75	96.96 ± 3.78
July 2007	96.79 ± 3.86	96.59 ± 4.02
	96.81 ± 3.88	96.84 ± 4.05

PDFs are still Gaussian but the means are -0.025 and -0.027 for January 2006 and January 2007, respectively, which are more deviated from zero compared to the nighttime cases.

One cautious note is that the regression coefficients (a_j, b) are indeed sensitive to the lower boundary temperature (i.e., surface temperature for a clear sky or cloud-top temperature for a cloud deck) and the total column water vapor. This is primarily because all six bands that we used as predictors are sensitive to the lower boundary temperatures, and many of them are also sensitive to water vapor continuum absorption. Therefore, to avoid intrinsic uncertainty associated with diurnal surface temperature, boundary layer, and cloud differences, it is desirable to choose observations over certain scene types of which surface temperature has small diurnal variations and, ideally, small interannual variations as well. A clear-sky oceanic scene is favored for these specific reasons. To minimize the impact of the seasonal cycle, we analyze data of the same month over different years in which the FM3 operated at the cross-track scanning mode. January and July are chosen and analyzed separately. Given the data availability and these constraints, observations over clear-sky oceans between 40°S and 40°N from two Januaries (2006 and 2007) and three Julys (2005, 2006, and 2007) are used for Edition 2 data analysis in this study (Edition 2 data were produced only up to 2007). For Edition 3 data, five Januaries (2006–10) and six Julys (2005–10) are available for analysis. Table 1 summarizes the means and standard deviations of I_{LW_CERES} in the above-mentioned months when both CERES Editions 2 and 3 data are available. As expected, the diurnal variation and interannual variation are both small ($\sim 1\%$ or even less). A seasonal difference $\sim 0.3\text{--}0.5 \text{ W m}^{-2} \text{sr}^{-1}$ exists in the I_{LW_CERES} between the January and July observations.

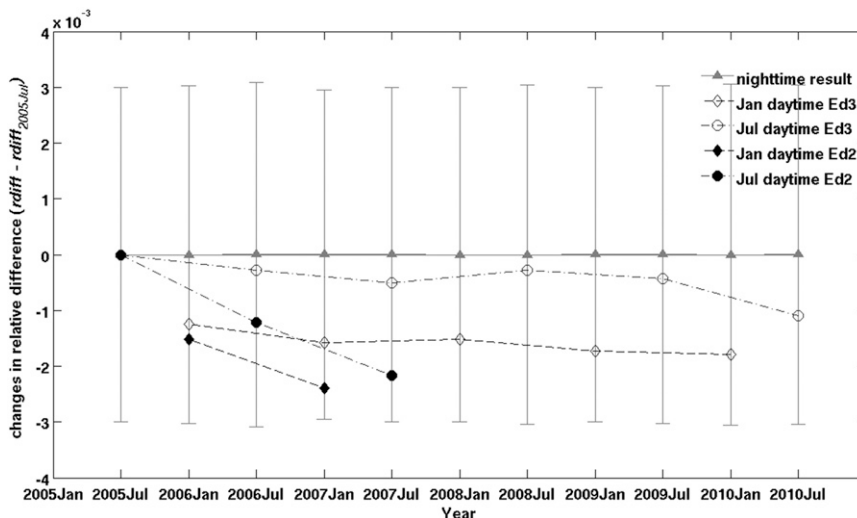


FIG. 3. The shift of mean rdiff with respect to the mean rdiff of July 2005 [please refer to Eq. (3) in the context for the definition of rdiff]. For nighttime, the changes are shown (filled gray triangles). The standard deviations of the nighttime rdiff of each month are represented (vertical bar). For the Julys, the shifts of daytime mean rdiff with respect to that of July 2005 are shown (circles) and for the Januaries, the shifts are also shown (diamonds); CERES Edition 2 (filled) and CERES Edition 3 (open) data are shown. CERES Edition 2 only has data up to 2007.

b. Results: Changes of rdiff with time

As described in section 2, rdiff and its PDF is calculated from daytime and nighttime observations in each month separately using the regression coefficients derived from the nighttime observations of the same month. Figure 3 summarizes the changes of mean rdiff over the period that we examine. As expected, the mean rdiff from the nighttime measurements changes little over time with respect to that of July 2005, the first data point in our analysis, as does the standard deviations of nighttime rdiff. As for the rdiff from daytime observations based on CERES Edition 2 data, the mean rdiff produced from three Julys from 2005 to 2007 drifts $-0.11\% \text{ yr}^{-1}$ and such drift is statistically significant (p value = 0.047)². The change of mean rdiff from January 2006 to January 2007 is -0.09% , similar to the drift seen in the July data. Note the mean rdiffs of Januaries have a systematic shift from that of the Julys, which is due to seasonal differences in temperature and water vapor that affect the regression parameters. Such $\sim -0.10\% \text{ yr}^{-1}$ changes for CERES Edition 2 data are consistent with the estimation by the

CERES calibration team (Priestley et al. 2011), which is $\sim -1.0\% \text{ decade}^{-1}$ based on nadir-view time series of all-sky LW unfiltered radiances over the oceans between 20°S and 20°N . Such drift is equivalent to a drift of $\sim 2.5 \text{ W m}^{-2} \text{ decade}^{-1}$ in OLR, which is much larger than the desired stability of the climate-quality OLR measurement [i.e., $\sim 0.2 \text{ W m}^{-2} \text{ decade}^{-1}$, see Ohring et al. (2005)]. The dominant reason for this secular drift is due to an incorrect adjustment to the SW portion of the TOT channel in the Edition 2 calibration, which adjusted all-sky radiances based on corrections derived from the scenes of deep convective clouds (Priestley et al. 2011). More detailed information about the corrections made in Editions 2 and 3 to the SW portion of the TOT channel can be found in LOE and Priestley et al. (2011).

Results based on CERES Edition 3 data (open circles and triangles in Fig. 3) have much smaller shift in daytime rdiff. The linear trend derived from the 5 yr of January data is $-0.012 \pm 0.0097\% \text{ yr}^{-1}$ [i.e., with the 95% confidence interval of the trend being $(-0.022\%, -0.0023\%) \text{ yr}^{-1}$]. Similarly, the July data yield a linear trend of $-0.016 \pm 0.015\% \text{ yr}^{-1}$. Both trends are much smaller than what are derived from the Edition 2 data (Fig. 2). This shows the improvements that CERES Edition 3 have achieved in correcting the secular drift of the shortwave sensor. Note that the shift of January results from the baseline 2005 July result is due to the intrinsic sensitivity of regression results to the surface temperature and lower-troposphere humidity. Hence,

² The drift and p value are derived from the linear regression of three July data points. In this case, the degree of freedom is only one but all linear regression statistics are still valid. The p value refers to the probability that a set of randomly selected three values would have a linear slope as large as the drift derived here (double-sided test).

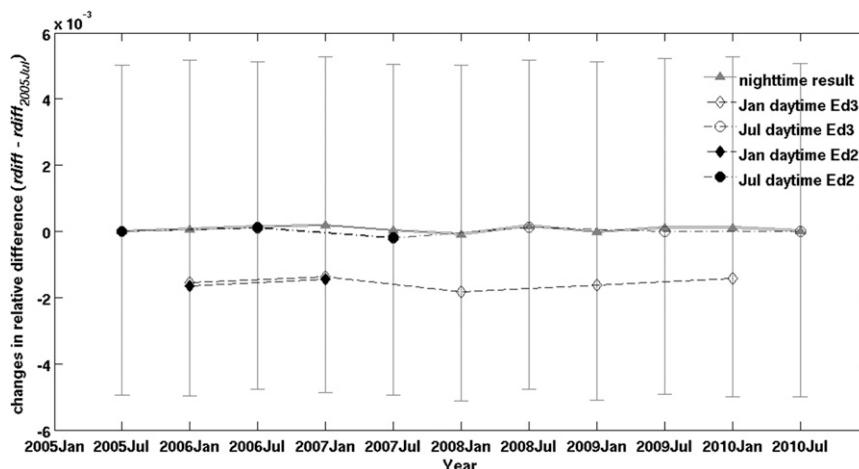


FIG. 4. As in Fig. 3, but for the window channel unfiltered radiances instead of the longwave unfiltered broadband radiances. The open and filled circles are largely overlapping with each other, so only the filled ones are clearly visible for July 2005–July 2007.

such a baseline difference between January and July does not change from CERES Edition 2 to Edition 3.

Given a typical value of daytime I_{LW_CERES} over the tropical clear-sky ocean being $\sim 97 \text{ W m}^{-2} \text{ sr}^{-1}$, the rdiff shift is equivalent to a drift of tropical clear-sky daytime LW radiance by $\sim -0.103 \text{ W m}^{-2} \text{ sr}^{-1} \text{ yr}^{-1}$ for CERES Edition 2 and $\sim -0.013 \text{ W m}^{-2} \text{ sr}^{-1} \text{ yr}^{-1}$ drift for CERES Edition 3. By assuming a simple Lambertian relation between radiance and flux, the upper bound of drift in daytime OLR is then $-0.32 \text{ W m}^{-2} \text{ yr}^{-1}$ for Edition 2 and $-0.041 \text{ W m}^{-2} \text{ yr}^{-1}$ for Edition 3. Tropical clear-sky OLR is usually larger than clear-sky OLR from other climate zones as well as the all-sky OLR. Therefore, these estimates can be deemed as the upper-bound estimates for the daytime OLR drift over the globe.

For comparisons, the rdiff statistics are calculated in the same way but are done so for the CERES window channel radiances and linear regression and predictions from radiances integrated over all AIRS window channels. The results are shown in Fig. 4 for both the Edition 2 and Edition 3 data. The results from two different editions are essentially identical for the window channel radiances, and no large drift is shown as the one for the case of Edition 2 on Fig. 3. As described in section 1, this is consistent with our expectation because no SW measurements are involved in the derivation of window channel radiance.

4. Conclusions and discussion

Utilizing the coincidental measurements from AIRS and CERES, we conducted a case study using spectrally resolved radiance to assess the secular drift in daytime CERES LW unfiltered radiances with respect to the

nighttime ones, as well as to assess how such drift has been addressed in different versions of broadband data products. A spectrometer with high spectral resolution, high calibration accuracy, and stable performance, such as AIRS, provides a new angle to assess such secular drift. A secular drift about $-0.10\% \text{ yr}^{-1}$ is identified for CERES Edition 2, which is consistent with other assessments using a different method. For the newly available CERES Edition 3, the drift is reduced to approximately -0.012 to $-0.016\% \text{ yr}^{-1}$. As long as the analysis and regression are carefully done (e.g., there is a selection of scene types with small diurnal variations and a selection of the same month each year to avoid seasonal fluctuation), then the amplitude of such drift can be assessed by using collocated AIRS and CERES measurements. We note here that the instrument trend would be nonlinear, though conventionally it is presented as a change of fixed value over a time interval (e.g., either per year or per decade). While previous studies established the synergy between AIRS and CERES in the detailed understandings of longwave flux and in evaluating climate models (Huang et al. 2008, 2010), this study shows the synergy of two measurements at the radiance level. An appropriate intercomparison of radiances from two instruments in an appropriate way could be informative and provide useful assessments for the instrument and its data products. While this study only focuses on the daytime drift relative to the nighttime CERES radiances, a similar method could be applied to a long-term AIRS and CERES time series to help evaluate the stability of the nighttime LW radiances over the years. This shall be the focus of our follow-up studies.

We attribute the majority of the drift shown in the Edition 2 data to the spectral degradation of the SW

component of the TOT channel resulting from the following facts: 1) As showed in Fig. 4, the WN channel does not show a discernible difference between daytime and nighttime observations. The WN radiance does not rely on the SW component of the TOT channel, and it is more sensitive to the surface temperature than the LW broadband radiance. As far as we know, there is no report or finding to show that the diurnal variability of ocean surface temperature has changed over the *Aqua* period. 2) The drift is largely removed in CERES Edition 3 in which the SW degradation effect has been corrected. These facts both support the attribution to the instrument issue instead of to any real physical long-term change in diurnal variability of sea surface temperature.

Acknowledgments. The first author wishes to thank Drs. G. Aumann, T. Pagano, and L. Strow for informative discussions on the AIRS radiance. We also wish to thank two anonymous reviewers for their thorough reviews and thoughtful comments. The research is supported by NSF ATM 0755310 and NASA NNX11AE68G awarded to the University of Michigan. The AIRS data were obtained from NASA GSFC DAAC and the CERES data from NASA Langley ASDC.

REFERENCES

- Aumann, H. H., and T. S. Pagano, 2008: Using AIRS and IASI data to evaluate absolute radiometric accuracy and stability for climate applications. *Atmospheric and Environmental Remote Sensing Data Processing and Utilization IV: Readiness for GEOSS II*, M. D. Goldberg et al., Eds., International Society for Optical Engineering (SPIE Proceedings, Vol. 7085), 8504–8504.
- , and Coauthors, 2003: AIRS/AMSU/HSB on the *Aqua* mission: Design, science objectives, data products, and processing systems. *IEEE Trans. Geosci. Remote Sens.*, **41**, 253–264.
- , S. Broberg, D. Elliott, S. Gaiser, and D. Gregorich, 2006: Three years of Atmospheric Infrared Sounder radiometric calibration validation using sea surface temperatures. *J. Geophys. Res.*, **111**, D16S90, doi:10.1029/2005JD006822.
- Chahine, M. T., and Coauthors, 2006: Improving weather forecasting and providing new data on greenhouse gases. *Bull. Amer. Meteor. Soc.*, **87**, 911–926.
- Ellingson, R. G., D. J. Yanuk, H.-T. Lee, and A. Gruber, 1989: A technique for estimating outgoing longwave radiation from HIRS radiance observations. *J. Atmos. Oceanic Technol.*, **6**, 706–711.
- Gaiser, S. L., H. H. Aumann, L. L. Strow, S. E. Hannon, and M. Weiler, 2003: In-flight spectral calibration of the atmospheric infrared sounder. *IEEE Trans. Geosci. Remote Sens.*, **41**, 287–297.
- Huang, X. L., and Y. L. Yung, 2005: Spatial and spectral variability of the outgoing thermal IR spectra from AIRS: A case study of July 2003. *J. Geophys. Res.*, **110**, D12102, doi:10.1029/2004JD005530.
- , W. Z. Yang, N. G. Loeb, and V. Ramaswamy, 2008: Spectrally resolved fluxes derived from collocated AIRS and CERES measurements and their application in model evaluation: Clear sky over the tropical oceans. *J. Geophys. Res.*, **113**, D09110, doi:10.1029/2007JD009219.
- , N. G. Loeb, and W. Z. Yang, 2010: Spectrally resolved fluxes derived from collocated AIRS and CERES measurements and their application in model evaluation: 2. Cloudy sky and band-by-band cloud radiative forcing over the tropical oceans over the tropical oceans. *J. Geophys. Res.*, **115**, D21101, doi:10.1029/2010JD013932.
- Lee, H.-T., A. Heidinger, A. Gruber, and R. G. Ellingson, 2004: The HIRS outgoing longwave radiation product from hybrid polar and geosynchronous satellite observations. *Adv. Space Res.*, **33**, 1120–1124.
- , A. Gruber, R. G. Ellingson, and I. Laszlo, 2007: Development of the HIRS Outgoing Longwave Radiation Climate Dataset. *J. Atmos. Oceanic Technol.*, **24**, 2029–2047.
- Loeb, N. G., P. O. Hinton, and R. N. Green, 1999: Top-of-atmosphere albedo estimation from angular distribution models: A comparison between two approaches. *J. Geophys. Res.*, **104**, 31 255–31 260.
- , K. J. Priestley, D. P. Kratz, E. B. Geier, R. N. Green, V. A. Wielicki, R. O. Hinton, and S. K. Nolan, 2001: Determination of unfiltered radiances from the clouds and the Earth's Radiant Energy System instrument. *J. Appl. Meteor.*, **40**, 822–835.
- , S. Kato, K. Loukachine, and N. Manalo-Smith, 2005: Angular distribution models for top-of-atmosphere radiative flux estimation from the Clouds and the Earth's Radiant Energy System instrument on the Terra satellite. Part I: Methodology. *J. Atmos. Oceanic Technol.*, **22**, 338–351.
- , B. A. Wielicki, F. G. Rose, and D. R. Doelling, 2007: Variability in global top-of-atmosphere shortwave radiation between 2000 and 2005. *Geophys. Res. Lett.*, **34**, L03704, doi:10.1029/2006GL028196.
- , —, T. Wong, and P. A. Parker, 2009: Impact of data gaps on satellite broadband radiation records. *J. Geophys. Res.*, **114**, D11109, doi:10.1029/2008JD011183.
- , S. Kato, W. Su, T. Wong, F. Rose, D. R. Doelling, and J. Norris, 2012: Advances in understanding top-of-atmosphere radiation variability from satellite observations. *Surv. Geophys.*, in press.
- Ohring, G., B. Wielicki, R. Spencer, B. Emery, and R. Datla, 2005: Satellite instrument calibration for measuring global climate change. *Bull. Amer. Meteor. Soc.*, **86**, 1303–1313.
- Pagano, T. S., H. H. Aumann, D. E. Hagan, and K. Overoye, 2003: Prelaunch and in-flight radiometric calibration of the Atmospheric Infrared Sounder (AIRS). *IEEE Trans. Geosci. Remote Sens.*, **41**, 265–273.
- Priestley, K. J., and Coauthors, 2011: Radiometric performance of the CERES Earth Radiation Budget climate record sensors on the *EOS Aqua* and *Terra* spacecraft through April 2007. *J. Atmos. Oceanic Technol.*, **28**, 3–21.
- Wielicki, B. A., B. R. Barkstrom, E. F. Harrison, R. B. Lee, G. L. Smith, and J. E. Cooper, 1996: Clouds and the Earth's Radiant Energy System (CERES): An earth observing system experiment. *Bull. Amer. Meteor. Soc.*, **77**, 853–868.
- Wong, T., B. A. Wielicki, R. B. Lee, G. L. Smith, K. A. Bush, and J. K. Willis, 2006: Reexamination of the observed decadal variability of the earth radiation budget using altitude-corrected ERBE/ERBS nonscanner WFOV data. *J. Climate*, **19**, 4028–4040.